Journal of Asian Scientific Research

journal homepage: http://aessweb.com/journal-detail.php?id=5003

OPTIMAL GAIN KALMAN FILTER DESIGN WITH DC MOTOR SPEED CONTROLLED PARAMETERS

Khalaf S. Gaeid

Electrical Engineering Department, Tikrit University, Tikrit, Iraq

ABSTRACT

The aim of this work, to design an appropriate Kalman filter(KF) with optimal gain as well as a two degree of freedom compensator for the DC motor, verify the stability of the proposed algorithm and the noise sensitivity are carried out. The design of the present algorithm is to combine both 2DOFPID controller with the optimal gain obtained by designing a (KF) to obtain better performance. The sensor noise covariance has been precisely chosen to design of the (KF) through state space model of DC motor. Controllability and observability are the main issues in the analysis of a system before deciding the best control strategy to be applied, or whether it is even possible to control or stabilize the system. Static parameters of a permanent magnet DC motor speed control with external load torque is simulated. The closed loop system and a two degree of freedom (2DOF) PID controller designed on the basis of the robust response tuning method. However, both no load and load current , speed and torque obtained. The (KF) speed response with the error between actual speed and estimated speed obtained. The robustness of the proposed algorithm checked through a 2DOF PID controller development. Comparison between classical PID speed response with 2DOF PID speed response carried out. The senses against the noise are approved as well as the torque and current in load and no load has been compared. The simulated results of the proposed algorithm improved performance operation and shows the effectiveness of the compensator new technique compared to the classical one.

Keywords: Kalman filter, Optimal gain, State space, Static parameter ,PWM, Bode plot, 2DOFPID controller

1. INTRODUCTION

The DC motor parameters given in the motor specifications are presented in Table 1.

Table- 1. DC motor specifications

Particulars	**Value**	**Unit**
Armature resistance	11.9	Ω
Armature inductance	0.3	H
Torque constant	14.8e-3	Km
Back emf constant (K_b)	14.8e-3	
Friction constant (K_f)	0.03	Nms
Moment of inertia(J)	0.045	kg.m2

The DC motor static parameters such as limb position and the isometric force states the motor cortical activity relationship and static conditions (Apostolos, 1999). Permanent magnet DC motors (PMDC) are used in a wide range of applications, such as battery powered devices, wheelchairs ,power tools, conveyors, door openers, welding equipment, and many other systems. Extensively the DC motors are used in position control and adjustable speed drive (ASD) applications.

Armature voltage controls the DC motor speeds below the base speed while field flux controls the speeds above the base speed. DC motors are preferred in speed control methods compared to AC motor due to their simplicity and less expensive, where wide speed range control is required (Anant Kumar *et al.*, 2007)

In the motion control and power transmission applications the DC motor is considered as the best solution due to a wide range of operating speed, compact size, their ability of adaptation of the power sources or the safety considerations. High torque production ability at low speed makes them a good alternative solution for gear motors in many applications. Their linear speed-torque curve, at less than 5000 RPM makes the DC motors suitable choice for the adjustable speed and servo control applications (Ronald Bullock, 1995).

New technique for speed control of a brushed DC motor without employing any direct shaft transducer in its feedback mechanism has been presented by (E Afjei *et al.*, 2007). The aim of a motor speed controller is to make the motor actual speed, equal to the reference speed. In the open loop scheme, the motor can be rotated at any given speed by controlling the time sequences between the PWM switching mechanism. This method is very easy and simple to implement but the absence of the feedback makes this method subjected to inaccurate switching at higher speeds. To solve the accuracy problem, the closed loop scheme is used where the back electromotive force (EMF) from the 3-Φ motor are frequently observed for the zero crossing (ZC) event. This due to the feedback from output to input to make the comparison between the switch sequences. The closed loop technique is highly accurate and will be a correction for any errors during the operation (Shanthamma and Nalini, 2012). DC motor PWM speed control, using microcomputers as controller, and the details of the realization of the approach based on AT89S51 single-chip microcomputer introduced by (Zhijun, 2011). The uses of digital signal processors (DSPs) such as TMS320F28335 and TMS320F2812 from Texas instrument (TI) have permitted the increasingly stringent performance requirements and fast, efficient, and accurate control of servomotor and motion control systems. DSPs are currently used for a wide range of control applications and communications (Gargees *et al.*, 2011). Fuzzy logic and proportional-integral-derivative (PID) controllers are compared to controlling the position of direct current (DC) motors done by (Arpit

Goel *et al.*, 2012). A model of the fuzzy PID control system is implemented in real time with a Xilinx FPGA to maintain a constant speed for a second order DC motor (Jose Luis, 2009). implementations of both PID digital control and (KF) algorithms as a necessary control for the direct inverted pendulum system(Meysam Shadkam *et al.*, 2013). In recent years, various methods are presented for auto tuning such as derivative based methods and derivative free methods. One of efficient derivative based methods is the (KF) (Basil Hamed and Moayed Al-Mobaied, 2011). Verification of the DC motor static parameters at load and no load ,develop a robust controller to minimize the noise sensitivity and ensure the closed loop system stability, less tuning time consuming of the developed two degrees of freedom PID controller to get optimal regulation and command tracking are the main contribution of this work.

The paper is organized as follows. In Section 2, we present the problem statement, and then we obtain the circuit implementation in Section 3. In Section 4, we present speed controller circuit, and present the pulse width modulation in Section 5. KF design is illustrated in Section 6.The simulation of the proposed approach is illustrated in Section 7, and the paper ends with some concluding remarks in Section 8.

2. PROBLEM STATEMENT

The (KF) is implemented to tune the PID. In fact, (KF) tries to estimate the proper state of the controller and used the updated ideal states in each step in order that the system performance will be improved. DC motors play a vital role in our lives. As the speed control technique is advanced, the current as an inner loop through the motor increases, but the voltage across the motor remains quite low. The control of the speed as outer loop has to be well regulated before the voltage and the power applied to the motor is high enough to overcome the reluctance increasing at starting. As the motor speed and the load on it changes from no load to full load conditions, there are changes in the motor internal resistance. Speed regulation design will be a very good choice especially in low voltage.

PWM is frequently used technique for the speed control to overcome the problem of the poor performance of motor at starting. Using Matlab/Simulink block to represent a wound field DC machine. The access is provided to the field terminals (F+, F-) so that the machine model can be used as a shunt connected or a series connected DC machine. The load torque applied to the shaft is provided at the Simulink input TL.

The armature circuit (A+, A-) consists of an inductor L_a and resistor R_a in series with a counter electromotive force (CEMF) which is labeled as E. The CEMF is proportional to the DC motor speed.

$$E = K_E \omega \qquad (1)$$

K_E is the voltage constant and ω is the machine angular speed. In a separately excited DC machine model, the voltage constant K_E is proportional to the field current I_f as in (2).

$$K_E = L_{af} I_f \qquad (2)$$

Where L_{af} is the field armature mutual inductance.

The electromechanical torque (T_e) developed by the DC machine is proportional to the armature current (I_a) as in (3).

$$T_e = K_T I_a \quad (3)$$

Where K_T is the torque constant. The sign convention for (T_e) and (T_L) is a positive in first and third quadrant (motor) and regenerative in the second and fourth quadrant (generator) as in (4) & (5).

$$T_e * T_L > 0 \quad motor \text{ mode} \quad (4)$$

$$T_e * T_L < 0 \quad generator \text{ mode}$$

(5)

In the SI unit, the torque and voltage constants are equal as in (6).

$$K_T = K_E \quad (6)$$

Series R_a L_a, controlled voltage source and a current measurement block configuration which represents the armature circuit is connected between the (A+,A-) terminals of the DC Machine block as can be illustrated in Fig.1.

Fig- 1. Armature circuit of DC motor

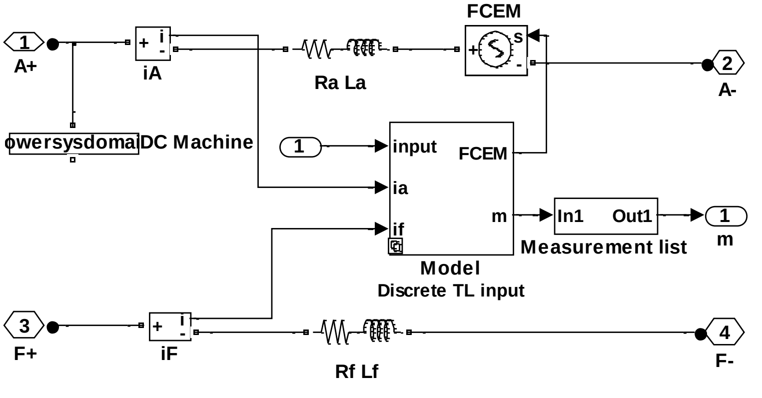

The mechanical circuit of the DC motor can be shown as in Fig.2.

Fig- 2. Mechanical configuration of the DC motor

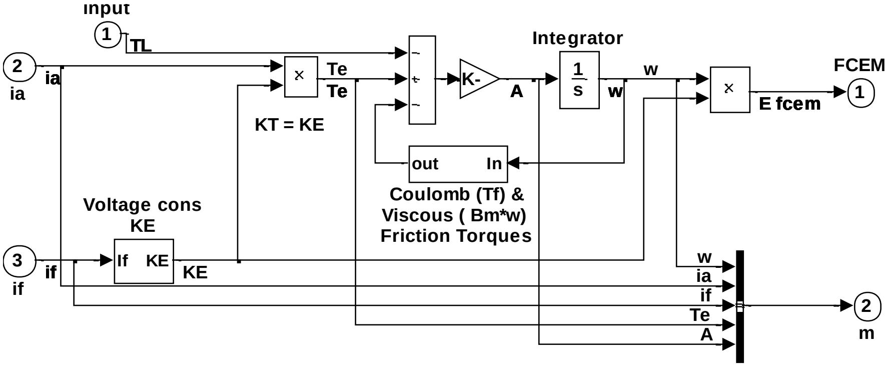

The field unit is represented by an RL circuit for the wound field DC machine model. It is connected between the (F+, F-) terminals of the DC motor block. In the permanent magnet DC machine model, there is no field current as the excitation flux is established by the magnets. K_E and K_T are constants.

The speed of the DC motor can be measured and computed from the resultant torques applied to the rotor.

The mechanical part can be represented and modeled using the Eq.7.

$$j\frac{d\omega}{dt} = T_e - T_l - B_m\omega - T_f \qquad (7)$$

Where *J*, B_m, and T_f are inertia, viscous friction coefficient, rotor speed and Coulomb friction torque respectively.

The state space model of the DC motor is:

$$\frac{d}{dt}\begin{bmatrix} i \\ \dot{\theta} \end{bmatrix} = \begin{bmatrix} -R/L & -K/L \\ K/J & 0 \end{bmatrix}\begin{bmatrix} i \\ \dot{\theta} \end{bmatrix} + \begin{bmatrix} 1/L \\ 0 \end{bmatrix} v \qquad (8)$$

In the sensorless methods, the measured outputs of the system is the measured current. Then, the output can be written as

$$i = [1 \;\; 0]\begin{bmatrix} i \\ \dot{\theta} \end{bmatrix} \qquad (9)$$

where i , v, $\dot{\theta}$ are the motor current, voltage applied ,speed of the motor (rad/sec) respectively. For simplicity, no load or friction torque will be assumed in this work .

After substituting the DC motor parameters listed in table 1, the system matrix (*A*), input matrix (*B*) and the output matrix(*C*) will be as follows:

$$A = \begin{bmatrix} -0.6667 & 0.3289 \\ -0.0493 & -39.667 \end{bmatrix}, \; B = \begin{bmatrix} 0 \\ 3.33 \end{bmatrix}, C = \begin{bmatrix} 1 & 0 \end{bmatrix}.$$

3. CIRCUIT IMPLEMENTATION

In industry applications, the PID controllers are widely used, but it is difficult for the conventional PID controller to achieve the expected action due to the noise interference. To increase the ability of the system to perform well both (KF) and 2DOFPID controller are used in one circuit. To satisfy both motor and generator ability in one configuration, four switch elements with their diodes and four quadrant chopper where the diodes are connected to anti parallel with the switching devices to ensure full bridge rectification topology. Fixed magnitude DC voltage (V_{dc}) is the input to the full bridge rectifier. The output of the rectifier can be a variable DC voltage with one polarity (positive or negative). According to the behavior, the circuit is called as four quadrant chopper circuit or DC to DC converter.

The inversion (inverter) is the second possibility output of the full bridge converter which is AC voltage with variable frequency and amplitude in which is a DC to AC conversion. Depending on the directions of the output load current either the switching device or the diode only will be conducted when a gating signal is given to a switching device in the full bridge converter a PWM converter can be used to allow a continuous speed variation of the motor (Ramesh, G.S., 2012).

4. SPEED CONTROLLER

For many years, the PID has been used for a control purposes. Due to its simplicity, robustness, a wide range of applicability and near optimal performance are some of the reasons that have made PID control so popular in the academic and industry applications (Cominos and Munro, 2002). The PID controller stands for parameters; the Proportional, the Integral and Derivative values. The proportional value (K_p) determines the reaction to the current error, the integral (K_i) determines the reaction based on the sum of recent errors or a reset action and the derivative (K_d) determines the reaction to the rate at which the error has been changed. The summing of all these actions is used to adjust the process via a control element such as the DC motor speed and position (Mohamad Farid Faruq, 2008). A PID controller attempts to correct the error between the actual process variable and a desired set point or the reference value of the variable by calculating, correcting action then adjust the process accordingly.

So by using the PID controller with the DC motor were able to compensate the error made by the DC motor and control the motor speed or the position to the desired position or speed.

The classical PID controller formula can be seen as in (10)

$$u_a = k_p e(t) + k_i e(t)/s + k_d e(t)s \qquad (10)$$

Unlike the PID Controller implementation, the two degrees of freedom PID Controller provides an extra degree of freedom to allow users to weight the set point (SP) as it passes through the proportional action channel and the derivative action channel. The SP weight c is chosen to be 0 to cancel undesirable transients upon a change in the SP, which is an effect known as derivative kick. The SP b affects the overshoot performance of the controller. A small b value reduces overshoot. Smaller b values can also result in sluggish response to set point changes (Astrom and Hagglund, 2005). The Simulink implementation of the developed 2DOF PID can be illustrated in Fig.3.

Fig- 3. Two degrees of freedom PID controller

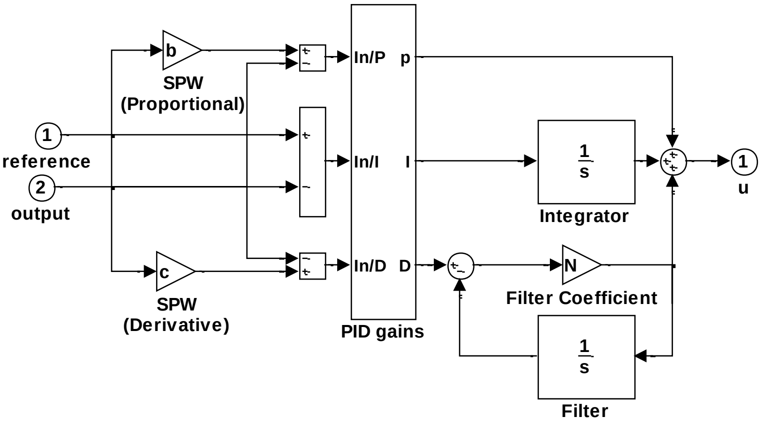

To design a robust PID controller ,the following steps should be considered (Ersin *et al.*, 2011):

• Determination of the transient response parameters and steady state error to improve the characteristics of the system.

The proposed closed loop system illustrated in Fig.4.

Fig- 4. Closed loop control system

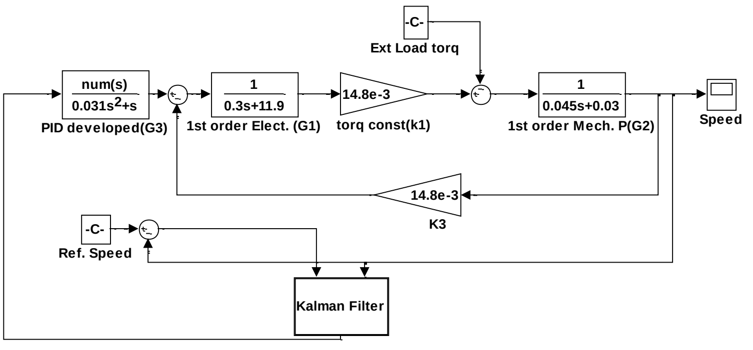

• K_P should be used to decrease the rise time.

• K_d should be used to reduce the overshoot and settling time.

• *Ki* should be used to eliminate the steady state error.

Tuning the PID controller with a robust response time algorithm to find the PID equation which is a tuning method to tune the PID gains to maximize bandwidth (BW) and optimize phase margin. The PID parameters have been chosen to satisfy less than 10% error between the reference speed and actual DC motor speed.

According to this, the PID transfer function will be as in (11).

$$C=\frac{57.24\,s^2+1039\,s+2756}{0.031s^2+s} \qquad (11)$$

And the plant transfer function (TF) obtained as in (12):

$$TF=\frac{0.1096}{s^2+11.33s+31.11} \qquad (12)$$

The 2DOFPID controller has been tuned through Kalman filter to get optimal performance with the optimal gain obtained from the (KF).

5. PULSE WIDTH MODULATION

Pulse width modulation (PWM) involves the modulation of its duty cycle (D), either:

1. Convey information over a communications channel or.
2. Control the amount of power sent to a load.

Pulse width modulation uses a square or triangle waveform whose pulse width is modulated resulting in the variation of the average value of the waveform. The duty cycle is defined as the percentage of digital 'high' to digital 'low' plus digital 'high' pulse-width during a PWM period

(Efy Lab, 2006). If we consider a modulated signal as a square waveform *f (t)* with a low value(y_{min}), a high value (y_{max}) and a duty cycle, the average waveform value is given by(13):

$$y = \frac{1}{T}\int_0^T f(t)dt \quad (13)$$

As stated earlier f (t) is a square wave, its value is (max) for high duty cycle and (min) for the lowest value of duty cycle. Eq.14 will be as follows:

$$y = D.y_{\max} + (1 - D).y_{\min} \quad (14)$$

Eq.13 can be simplified in many cases, one of them make $y_{min} = 0$. According to that, the average value (y) will be directly related to the duty cycle. The simplest way to generate a PWM signal is the intersection method, which requires only modulated signal and a comparator. When the value of the reference signal is more than the modulation waveform, the PWM signal is in the high state, otherwise it is in the low state as can be seen in Fig.5.

Fig- 5. Pulse width generation circuit

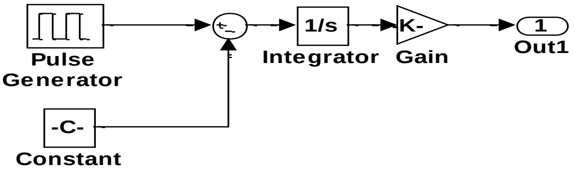

Controllability and observability are main issues in the analysis of a system before deciding the best control strategy to be applied, or whether it is even possible to control or stabilize the system. Controllability is related to the possibility of forcing the system into a particular state by using an appropriate control signal. If a state is not controllable, then no signal will ever be able to control the state. If a state is not controllable, but its dynamics are stable, then the state is termed stabilizable. Observability instead is related to the possibility of "observing", through output measurements, the state of a system. If a state is not observable, the controller will never be able to determine the behavior of an unobservable state and hence cannot use it to stabilize the system. However, similar to the stabilizability condition above, if a state cannot be observed it might still be detectable (hps project, 2001). To check controllability of the system the following Matlab instruction has been used.

$$[A_{bar}, B_{bar}, C_{bar}, T, k] = ctrbf(A, B, C) \quad (15)$$

$$A_{bar} = [-3.9685 \quad -11.0432; -10.6710 \quad -36.3655]$$

$$B_{bar} = [0; 3.4769]$$

$$C_{bar} = [-0.9577 \quad 0.2876]$$

Where A_{bar}, B_{bar}, and C_{bar} decomposes the state space system represented by *A*, *B*, and *C* into the controllability staircase form.

$T = [-0.9577 \ \ 0.2876; 0.2876 \ \ \ 0.9577]$

T is the similarity transformation matrix

$K = [1 \ \ 1]$

k is a vector of length 2, which is same as of the order of the system represented by *A*. Each entry of *k* represents the number of controllable states factored out during each step of the transformation matrix calculation. The number of nonzero elements in k indicates how many iterations were necessary to calculate *T*, and sum(*k*) is the number of states in *A*C*, the controllable portion of Abar.To check the observability, the following equation will be used.

$$[A_{bar}, B_{bar}, C_{bar}, T, k] = 0bscf(A, B, C) \tag{16}$$

$A_{bar} = [-39.6670 \ \ -0.0493; 0.3229 \ \ \ -0.6670]$

$B_{bar} = [\ 3.33; 1]$

$C_{bar} = [\ 0 \ \ \ 1]$

$T = [0 \ \ \ 1; 1 \ \ \ 0]$

$K = [1 \ \ 1]$

The system is controllable and observable for all periods of operation.

6. KALMAN FILTER DESIGN

KF has numerous applications in technology. A common application is for guidance, navigation and control of vehicles, particularly aircraft and spacecraft. Furthermore (KF) is a widely applied concept in time series analysis used in fields such as signal processing and Econometrics (James, 1994). (KF), also known as linear quadratic estimation (LQE), is an algorithm that uses a series of measurements observed over time, containing noise (random variations) and other inaccuracies, and produces estimates of unknown variables that tend to be more precise than those based on a single measurement alone. More formally, (KF) operates recursively on streams of noisy input data to produce a statistically optimal estimate of the underlying system state (Kalman, R. E., 1960). Filter works, generate some data and compare the filtered response to the true plant response as can be seen in Fig.6.

Fig- 6. Kalman filter and plant configuration

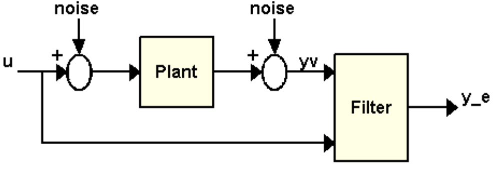

To design (KF) ,the following parameters or weighting matrices should be specified through a trial and error process (Karl and Richard, 2008)

Q = 2.2;

R = 0.9

Where Q , R is the sensor noise covariance and number greater than zero respectively.

Using Matlab to design a (KF) as in (17):

$$[kalman, L, \sim, M, Z] = kalman(plant, Q, R) \quad (17)$$

The first output of the Kalman filter KALMF is the plant output estimate as follows:

$$y\_e = Cx[n|n] \quad (18)$$

The remaining outputs are the state estimates and M is the optimal innovation gain

The optimal gain according to the (KF) is :

$M = [0.5345; 0.0101; -0.4776]$

The block diagram of the combined 2DOFPID and the (KF) can be illustrated in Fig.7

Fig-7. Block diagram of the proposed algorithm

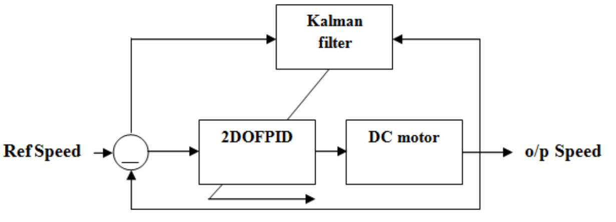

7. RESULTS AND DISCUSSION

After Simulink implantation of the proposed(KF) with the 2DOFPID controller and all the circuit units, the DC motor starts its rotation at armature voltage of 1 Volt approximately as can be seen in Figs (8,9,10) then the speed follows the voltage linearly. An approximately equal counter EMF must be generated for every voltage which is applied externally to the motor. This counter EMF results from the strength of the constant motor field and speed. The speed is therefore locked to the armature voltage (Sharifian *et al.*, 2009). The DC motor armature load and no load current (within 25 m A) are plotted against the variation of armature voltage (0-6) Volt as shown in Fig.8.

Fiq- 8. Load and no load currents of DC motor

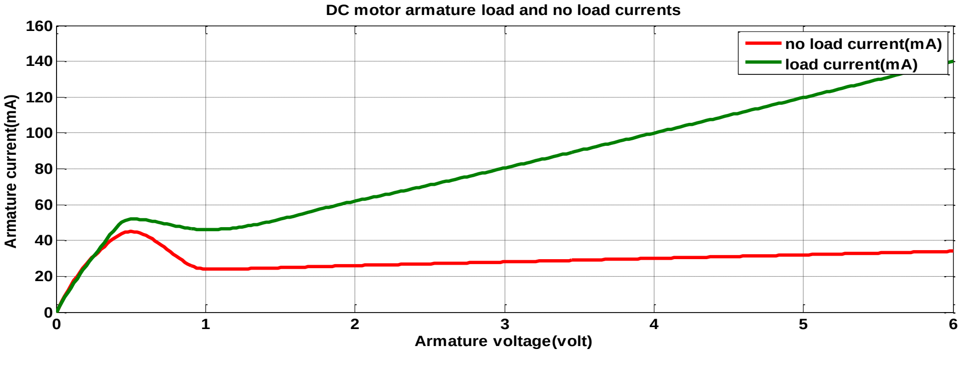

Fig.9. Shows the DC motor no load and loaded speed with an external torque of 0.5 mN.m when the voltage (0-6) Volt.

Fig- 9. Load and no load speed versus armature voltage

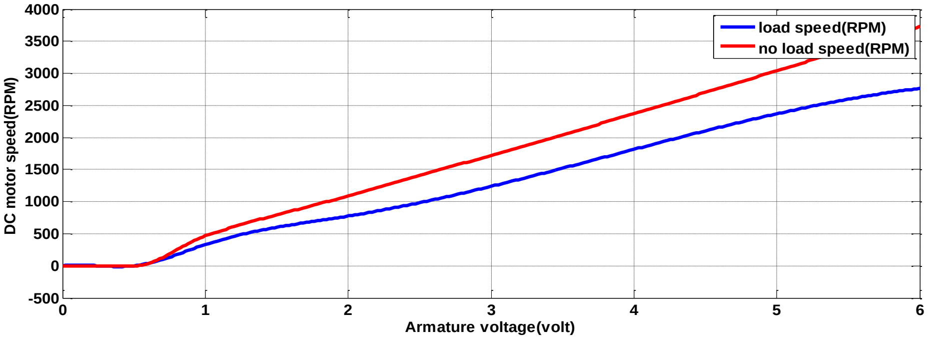

The no load and load torque comparison under different DC motor armature voltage can be shown in Fig.10.

Fig- 10. No load and load torque against voltage variation.

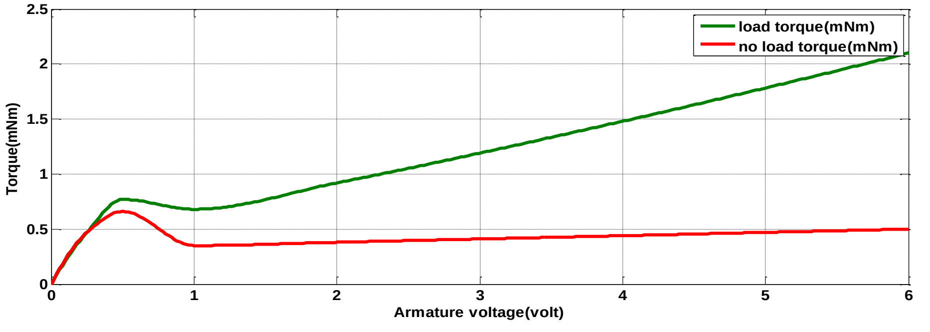

The robustness of the proposed algorithm checked through a developed compensator and the sensitivity against the noise as shown in Fig.11.

Fig.11. Shows the Bode plot of both compensatory and the noise sensitivity.

Fig- 11. Bode plot of noise sensitivity and compensator

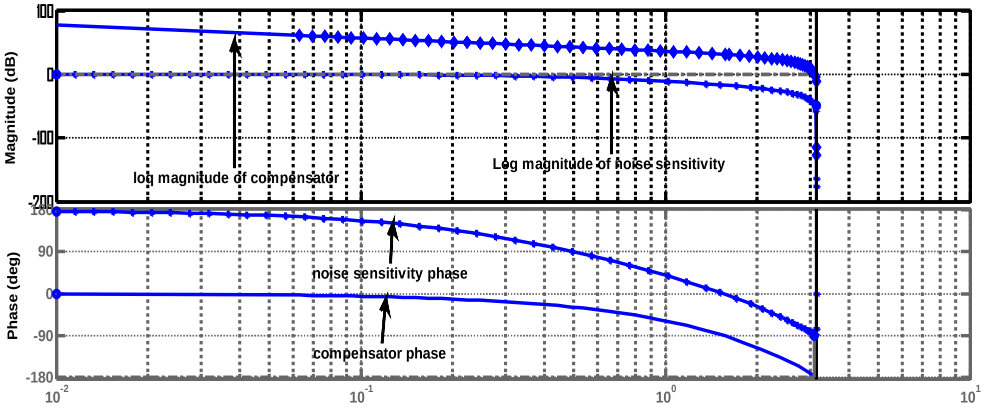

From the Bode plot (logarithmic magnitude and phase), both phase margin and gain margin of the noise sensitivity and the compensator are positive so that the system is stable (Julier and Uhlmann, 1997) Fig.12 shows the Loaded and no load speed response.

Fig- 12. Load and no load speeds of versus the time

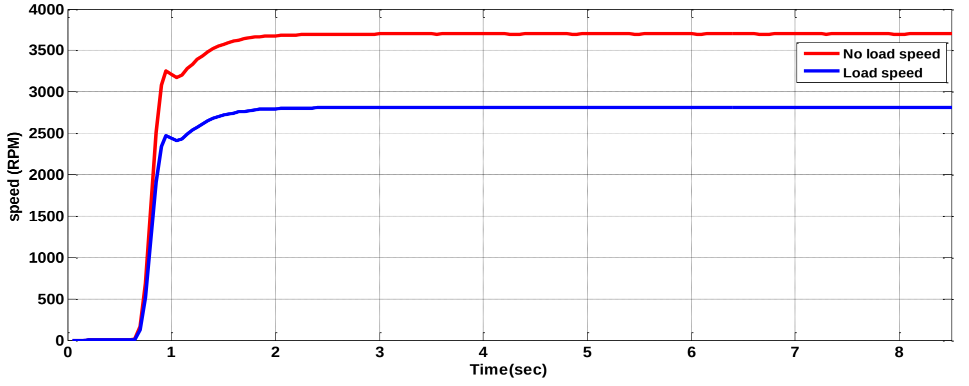

The actual motor speed is compared to the reference speed. The actual speed with error obtained will be as input to the kalman filter to estimate the optimal state and tune the 2DOF PID controller get the actual speed equal to the set point or reference speed. This creates a cycle where the motor's speed is frequently being checked against the desired speed. The results prove the control system robustness and the two degrees of freedom PID so efficient compared to the classical PID especially in tune time consuming (Khalaf *et al.*, 2013) as in Fig.13.

In this figure, better regulation and tracking of the speed reference can be obtained with a 2DOF PID tuned by (KF) compared to classical PID and 2DOFPID controllers.

Fig- 13. Reference and actual speed response

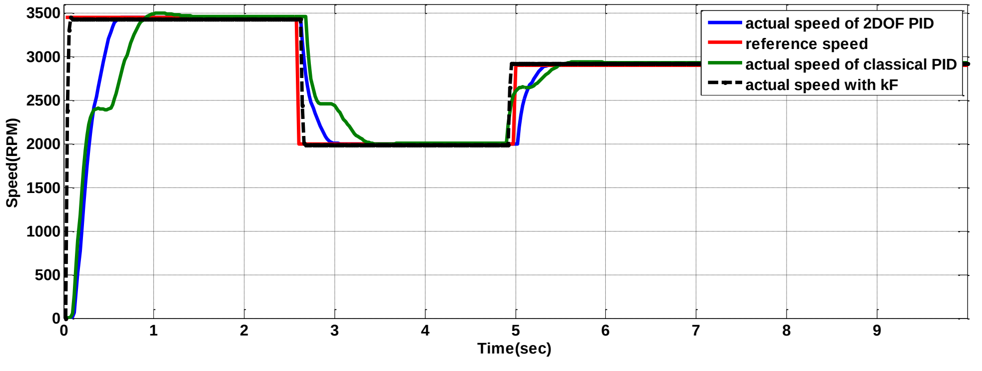

The (KF) speed response with the error between actual speed and estimated speed (y to y_e) (Garcia *et al.*, 2005) can be illustrated as can be seen in Fig.14.

Fig- 14. Kalman filter output response (above) with the error (below)

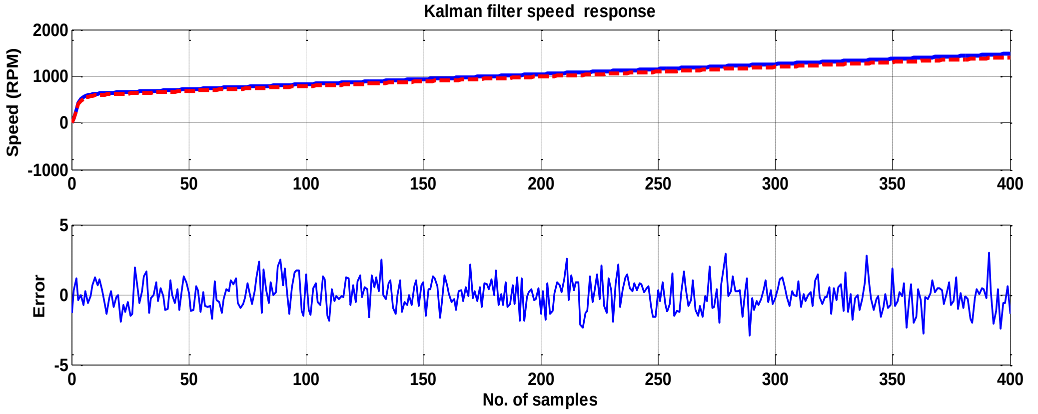

The error between (u to y_e) speeds according to the (KF) can be illustrated in Fig.15

Fig- 15. Kalman filter output response (above) with the error (below)

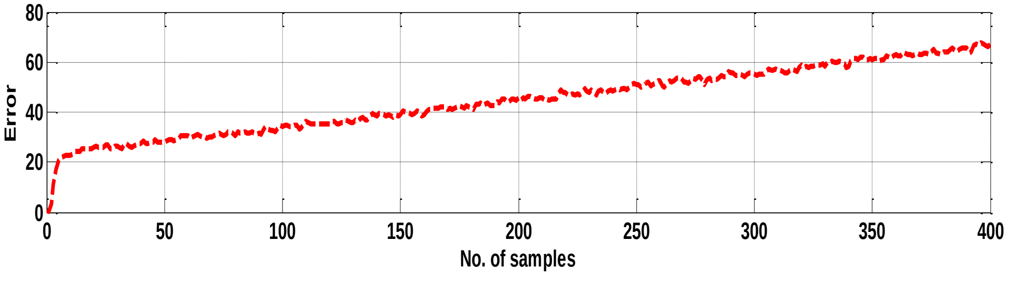

To investigate the robustness of the (KF) design ,Bode plot of the system (u to y_e) and (y to y_e) configuration can be shown in Fig.16.

Fig- 16. Bode plots of the Kalman filter

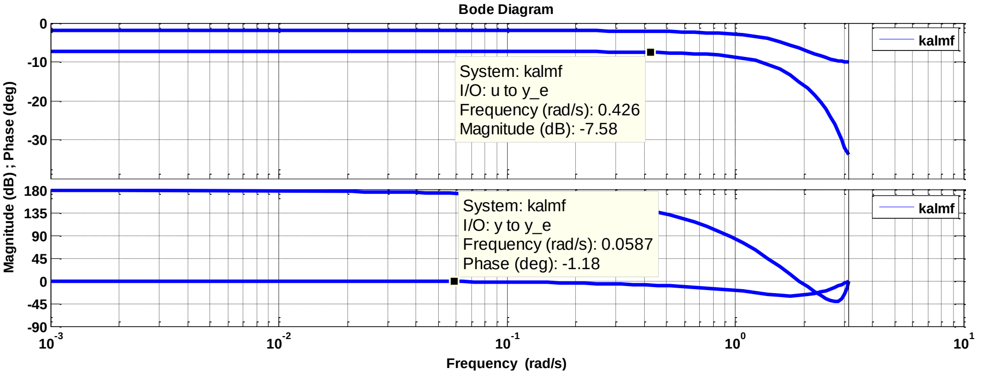

Fig- 17. Simulink implementation of the proposed algorithm.

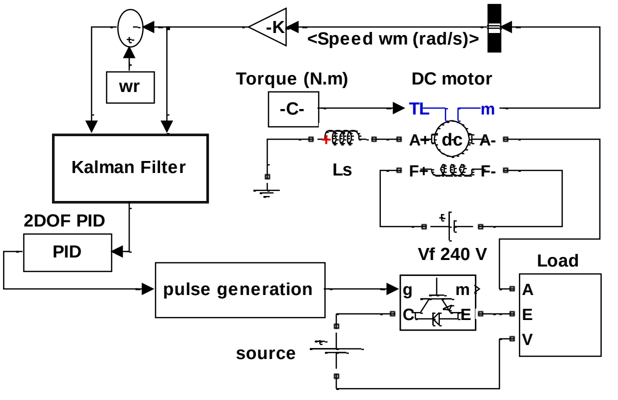

8. CONCLUSION

The design of DC motor speed system using both optimal gain control through (KF) and 2DOFPID have been presented in this paper. The static parameters can be obtained when the input voltage can be applied directly through a potentiometer. The motor starts rotating at an armature voltage near to 1Volt. As soon as the static friction in the bearings has been overcome by producing torque, the armature rotates and electromotive force is generated which reduces the current, hence the speed of the motor is loaded. When the motor with no load, the current is necessary to overcome the friction torque in the bearing. 2DOF PID controller has been developed to be one of the powerful support of this algorithm.

9. ACKNOWLEDGEMENTS

I am grateful to Prof. Hew Wooi Ping , UMPEDAC excellent center, University of Malaya for his valuable guidance and encouragement and for financial assistance, I am also thankful to Prof. Faisal Rafiq ,Prof. Nasir Uddin and Prof. Parry William for their co-operation throughout the study period.

REFERENCES

Anant Kumar, Mohammed Rehan Memon, Shreerang Pradeep Munshi and S. Mishra, 2007. Speed control of DC motor using IGBT. National Institute of Technology. Rourkela.

Apostolos, P.G., 1999. News in motor cortical physiology. Physiology, 14(2): 64-68.

Arpit Goel, Ankit Uniyal, Anurag Bahuguna, R.S. Patwal and H. Ahmed., 2012. Performance comparison of pid and fuzzy logic controller using different defuzzification techniques for positioning control of dc motors. Journal of Information Systems and Communication, 3(1): 235-238.

Astrom, K. and T. Hagglund, 2005. Advanced PID control, ISA, Research Triangle Park, NC, August.

Basil Hamed, H. and Moayed Al-Mobaied, 2011. Fuzzy pid controllers using FPGA technique for real time DC motor speed control. Scientific Research., 2(3): 233-240.

Cominos, P. and N. Munro, 2002. Pid controllers: Recent tuning methods and design to specification. IEE Proceedings Control Theory and Applications, 149(1): 46-53.

E Afjei, A., G. Nadian and A. Karami, 2007. Sensorless speed/position control of brushed DC motor. International Aegean Conference on Electrical Machines and Power Electronics, ACEMP: 730-732.

Efy Lab, 2006. Speed control of DC motor using pulse-width modulation. 97. Available from www.efy mag.com.

Ersin, Y., A. Serkan and E. Metin, H. , 2011. Real time dsp based pid and state feedback control of a brushed dc motor. International Symposium on Information, Communication and Automation Technologies (ICAT): 1-6.

Garcia, O., Cesar; and C. Fyfe, 2005. Visualization of high dimensional data via orthogonal curves. Journal of Universal Computer Science, 11(11): 1806-1819.

Gargees, R.S., A.K.Z. Mansoor and R.A. Khalil, 2011. Dsp based adjustable closed loop DC motor speed control system. Al-Rafidian Engineering, 19(5): 66-76.

HPS project, C.S.C.C., 2001. Technical report, hps system technique.

James, D.H., 1994. Time series analysis. Princeton University Press.

Jose Luis, C.M., 2009. Application of kalman filtering and pid control for direct inverted pendulum control. Degree Master of Science in Electrical and Computer Engineering. California State University, Chico.

Julier, S.J. and J.K. Uhlmann, 1997. A new extension of the kalman filter to nonlinear systems. Int. Symp. Aerospace/Defense Sensing, Simul. and Controls 3. Proc. SPIE, 3068: 182-193.

Kalman, R.E. 1960. A new approach to linear filtering and prediction problems. Transactions of the ASME–Journal of Basic Engineering, 82 (Series D): 35-45.

Karl, J.A. and M.M. Richard, . 2008. Feedback systems: An introduction for scientists and engineers. Princeton University Press.

Khalaf, S., Gaeid,, A.H. Jamal, M. Hameed Ali and K.H. Mohammed, 2013. Static DC motor speed controlled parameters correction. British Journal of science and Technology, 3(3): 586-597.

Meysam Shadkam, Hamed Mojallali and Y. Bostani., 2013. Speed control of DC motor using extended kalman filter based fuzzy pid. International Journal of Information and Electronics Engineering, 3(1): 109-112.

Mohamad Farid Faruq, 2008. Pid controller design for controlling DC motor speed using matlab application. Faculty of Electrical & Electronics Engineering University Malaysia Pahang.

Ramesh, G.S., 2012. Introduction to four quadrant chopper drive for Dc motor electronics project: 1-4.

Ronald Bullock, 1995. Applying pmdc motors. Bison Gear & Engineering Corp: 33-36.

Shanthamma, Y.T. and S. Nalini, 2012. Modeling and simulation of real time electronic speed controller of position sensorless brushless DC motor. International Journal of Engineering Research & Technology (IJERT), 1(4): 1-3.

Sharifian, M.B.B., R. Rahnavard and H. Delavari, 2009. Velocity control of DC motor based intelligent methods and optimal integral state feedback controller. International Journal of Computer Theory and Engineering, 1(1): 1793-8201.

Zhijun, L., 2011. PWM speed control system of DC motor based on at89s51. In: International Conference on Electronic and Mechanical Engineering and Information Technology (EMEIT). pp: 1301-1303.